Diffusion Model-based Signal Recovery in Coexisting Satellite and Terrestrial Networks

Abuzar B. M. Adam, Mostafa Samy, Carla E. García, Eva Lagunas, Symeon Chatzinotas
Interdisciplinary Centre for Security, Reliability and Trust (SnT), University of Luxembourg
E-mails: {abuzar.babikir, mostafa.samy, carla.garcia, eva.lagunas, symeon.chatzinotas}@uni.lu

***Abstract*—Coexisting satellite and terrestrial networks present a unique set of challenges and opportunities when the two networks share the same spectrum. One of these challenges is the signal recovery. In this work, we design a signal recovery scheme in coexisting satellite and terrestrial networks. We formulate an optimization problem and propose a diffusion model to perform signal recovery. The proposed diffusion model leverages the denoising mechanism to recover the signals from noisy and distorted signals. The proposed diffusion model consists of encoder to encode the input to the latent space, U-Net for denoising, attention block to integrate different relevant feature to create better context for signal recovery, and decoder to deliver the recovered signal.**

***Index Terms*—Satellite network, terrestrial network, low earth orbit (LEO) satellite, Diffusion model, signal recovery.**

I. Introduction

Coexistence of satellite and terrestrial networks represent a complex and dynamic aspect of modern communication systems. Working together, satellite and terrestrial networks can ensure comprehensive coverage, combining the wide reach of satellite networks with the high capacity and low latency of terrestrial networks [1]. Nevertheless, major challenges in these networks include managing interference between satellite, equipment noises, and terrestrial signals and recovery of these signals, especially in bands where both systems operate [2], [3]. Traditional methods such as power amplifier linearization techniques have been widely used [4]. The premise of these traditional methods is that the working conditions of the power amplifier need to be maintained to obtain a stable operating state. Despite the typically robust design of satellite transmission systems, minor fluctuations in signal levels and power supplies may still occur, owing to the severity of the irradiation environment they operate in [5].

Traditional communication systems rely on handcrafted algorithms and models for signal prediction. However, with the advent of deep learning, there has been a paradigm shift towards data-driven approaches that leverage the power of deep neural networks (DNNs) to automatically learn complex patterns and representations from large amounts of data. In this context, deep learning-based signal recovery concept is consistent with this direction of the technology development. Benefiting from the robustness to noise provided by the deep neural networks (DNN) themselves [4], [6], [7] and the power independence contributed by batch normalization (BN) layers, the proposed concept is becoming possible.

This work is financially supported by the Luxembourg National Research Fund (FNR) under the project SmartSpace (C21/IS/16193290).

Generative deep learning for signal recovery is a cutting-edge approach that leverages the power of generative models such as generative adversarial networks (GANs) and autoencoders such as variational autoencoders (VAEs) to reconstruct or enhance signals that have been degraded or distorted [8]. Different from these generative models, diffusion models work by gradually learning to reverse a diffusion process, which gradually adds noise to the data until it turns into a random noise signal. The model is trained to do the opposite: starting from noise, it learns to gradually reconstruct the original data. Motivated by the above working mechanism the diffusion models, we propose a diffusion model-based signal recovery scheme for coexisting satellite and terrestrial networks with large LEO satellite constellation. To the best of our knowledge, this the first work to use employ diffusion model to perform signal recovery in satellite communications. The contributions of this work can be summarized as follows:

- We consider coexisting satellite and terrestrial networks. The satellite network consists of low earth orbit (LEO) satellite constellation modelled as cell-free MIMO serving multiple satellite users (SUs). The terrestrial network consists of multiple base stations (BSs) causing interference to the SUs. Aiming at recovering the signal at the SUs, we formulate an optimization problem.
- To handle the formulated problem, we propose a diffusion model-based signal recovery scheme. The proposed model leverages the denoising mechanism to recover the signals from noisy and distorted signals. The proposed diffusion model consists of encoder to encode the input to the latent space, U-Net for denoising, attention block to integrate different relevant feature to create better context for signal recovery, and decoder to deliver the recovered signal.
- We compare the performance of the proposed scheme with recent work in the literature and we show that the proposed scheme has superior performance.

II. System Model and Problem Formulation

Fig. 1 illustrates satellite and terrestrial networks coexisting on the same spectrum and consist of LEO satellite constellation (LEO SatCon) consists of L satellites serving K_s satellite users (SUs) and B base stations (BSs) serving K_c cellular users (CUs). Each LEO satellite s, SU k_s, and BS b are

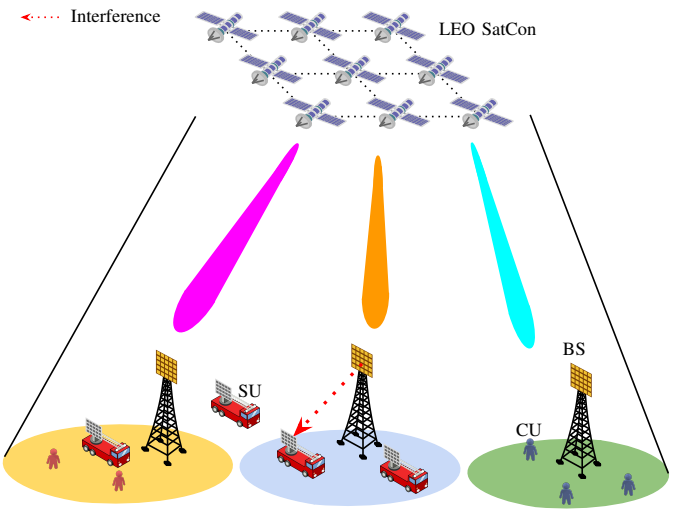

Fig. 1. Schematic diagram of network architecture of coexisting terrestrial and LEO satellite constellations networks.

equipped uniform planar array (UPA) respectively denoted as $M = M_x \times M_y$, $N = N_x \times N_y$, and $A = A_x \times A_y$.

A. Channel Model

To model the propagation and attenuation where the path loss components, the channel model includes the large-scale fading and the small-scale fading. The large-scale fading between the satellite and SUs. [9]

$$PL_{Tot} = PL_b + PL_g + PL_s, \tag{1}$$

where PL_b represents the basic path loss, PL_g accounts for the attenuation due to atmospheric gasses, PL_s is the attenuation due to either ionospheric or tropospheric scintillation. All these path loss components measured in dB. Specifically, the basic path loss model PL_b accounts for the signal's free space propagation and shadow fading. The free space path loss (PL_{FS}) in dB for a distance $d_{k,i}$ (also known as slant range) in meter and frequency f_c in GHz. Hence, the slant distance $d_{k,i}$ can be expressed in terms of the satellite altitude H and its elevation angle as [10], [11]:

$$d = \sqrt{R_e^2 \sin^2\theta + r_m^2 + 2R_e r_m} - R_e \sin\theta, \tag{2}$$

where $R_E = 6378$ Km is the radius of the Earth, r_m, and θ, are the satellite altitude and its elevation angle, respectively. Thereby, the free space path loss (PL_{FS})can be calculated as:

$$PL_{FS}(d, fc) = 32.45 + 20\log_{10}(fc) + 20\log_{10}(d). \tag{3}$$

Shadow fading (SF) is modeled by a log-normal distribution as $\sim \mathcal{LN}(0, \sigma_{SF}^2)$ with zero-mean and σ_{SF} standard deviation. The values of σ_{SF}^2 can be extracted from the 3GPP Release-15. Then, the path loss with shadow fading in dB units is modeled as:

$$PL_b = PL_{FS}(d, fc) + SF. \tag{4}$$

The large-scale fading effects of the LEO satellite s to the SU k_s after considering the LEO satellite antenna gain G_T can be modeled as

$$\zeta_{s,k_s}(dB) = PL_{Tot} - G_T. \tag{5}$$

B. Small Scale Channel Model

In this work, we focus on the case where both line-of-sight (LoS) and non-LoS (NLoS) paths of the LEO satellite channels exist [11], [12]. Small-scale fading consists of line-of-sight (LoS) and non-LoS (NLoS) components. Accordingly, we consider the Rician model to express the channel between LEO satellite s and the SU k_s. The channel from the LEO satellite s to the SU k_s is given as

$$\mathbf{f}_{s,k_s} = \sqrt{\frac{R_k \zeta_{s,k_s}}{R_k + 1}} \bar{\mathbf{f}}_{s,k_s} + \sqrt{\frac{\zeta_{s,k_s}}{R_k + 1}} \tilde{\mathbf{f}}_{s,k_s}, \tag{6}$$

where $\bar{\mathbf{f}}_{s,k_s}$ and $\tilde{\mathbf{f}}_{s,k_s}$ are the LoS and NLoS components, respectively, and R_k is the Rician factor. Further, the entries of $\tilde{\mathbf{f}}_{s,k_s}$ are independent and identically distributed (i.i.d.) and follow the complex Gaussian distribution with zero mean and unit variance. Given that users are often separated by only a few wavelengths, it can be assumed that the channel realizations from the satellite to various users uncorrelated. Consequently, by employing a ray-tracing based channel modeling method, the complex baseband downlink space domain channel at a time instance t and frequency f can be depicted as [9]

$$\mathbf{h}_{s,k_s}(t, f) = \sum_{u_{k_s}=1}^{U_{k_s}-1} \mathbf{f}_{s,k_s} . \exp\left(2\pi\left[t\nu_{k_s} - f\tau_{k_s}\right]\right) \tag{7}$$

where U_{k_s} is the number of propagation paths of the SU k_S, ν_{k_s} is the doppler shifts, and τ_{k_s} is the propagation delay.

C. Signal Model

In the considered downlink data transmission scenario, linear precoding is executed at the LEO satellite s for transmitting data to the K SUs who are concurrently served on the same time-frequency blocks. The received signal at the SU k_s is given as

$$y_{k_s} = \underbrace{\sum_{s=1}^{S} \mathbf{h}_{s,k_s}^H x_{s,k_s}}_{\text{Desirable signal}} + \underbrace{\sum_{i_s \neq k_s}^{K_s} \sum_{s=1}^{S} \mathbf{h}_{s,i_s}^H x_{s,i_s}}_{\text{Inter - user interference}} + \underbrace{I_{\text{tr}}}_{\text{Terrestrial interference}} + \underbrace{z_{k_s}}_{\text{Noise}}, \tag{8}$$

where x_s represents the transmit signal at satellite s. The interference from the coexisting terrestrial network I_{tr} is estimated at SU k_s assuming that the satellite network has no information on the terrestrial network. $z_{k_s} \sim \mathcal{CN}\left(0, \sigma_k^k\right)$ is the additive white Gaussian noise (AWGN) at SU k_s.

Let us denote the desirable signal of SU k_s as d_{k_s}. Recovering d_{k_s} perfectly can be challenging, which may always lead to a residual loss. Although the residual loss may be negligible compared with d_{k_s}, but still resulting in an incorrect estimation of d_{k_s}. To address this issue of recovering d_{k_s}, signal detection problem is formulated as follows [13]

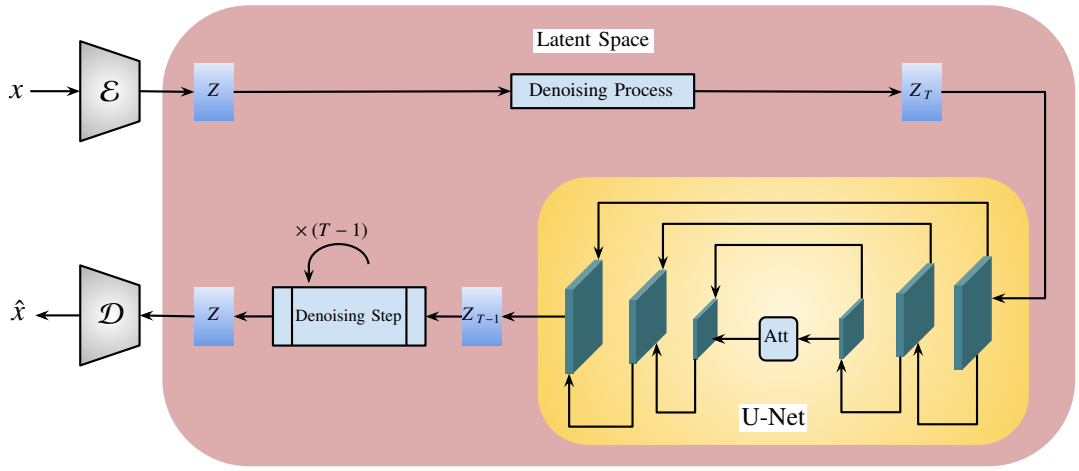

Fig. 2. Architecture of the proposed diffusion model.

$$\min_{\theta} \quad \mathcal{L}(\theta) = \mathbb{E}\left\{\left\|d_{k_s} - \hat{d}_{k_s}\right\|^2\right\} \tag{9}$$

$$\text{s.t.} \quad \hat{d}_{k_s} = \mathcal{F}_\theta(d_{k_s}), \tag{9a}$$

where θ is the parameters of the recovery model, $\hat{d}_{k_s}$ is the detected signal, and $\mathcal{F}_\theta(d_{k_s})$ is proposed signal receovery model. In the following section, we propose the signal recovery model.

III. Diffusion Model for Signal Recovery

In this section, we present the details of the proposed diffusion model-based scheme signal recovery. Before diving into the structure, it's important to understand that diffusion models work by gradually transforming a sample of random noise into a structured output through a series of learned reverse diffusion steps [14], [15]. To adapt this concept to our data (which is numerical data), we would essentially be training a model to "denoise" numerical data, iteratively refining random or noisy numerical inputs into cleaner, structured outputs which represent the predicted channels and recovered signals.

A. Model Architecture

The proposed diffusion model depicted in Fig. 2 operates by using a process known as "diffusion modeling," which is a generative technique that involves a forward "diffusion" process to add noise to input data, and a reverse "denoising" process to reconstruct the data. Below we explain the architecture and working mechanism of the model:

- Encoding to Latent Space: The process begins with an original input signal X that is encoded into a latent space representation z using an encoder $\mathcal{E}$. The latent space is typically a lower-dimensional representation of the input signal, which includes the necessary features for the signal reconstruction.
- Diffusion Process: Once the input signal is in the latent space, diffusion process is applied on the input signal. This process gradually adds noise over a series of discrete time steps T, transforming the data into a completely noised version z_T by the final time step. Using a known method in advanced, we add the noise according to a predefined noise schedule.
- Denoising with U-Net: The reverse process involves a denoising U-Net, which is an efficient DNN. The U-Net is trained to predict the original input signal from the noised latent representation. U-Net predict the original signal by iteratively denoising the latent representation across the time steps from T to 1.
- Attention Mechanisms: Inside the U-Net, there is a block that utilizes attention mechanism. This mechanism allows the network to focus on and integrate relevant features across different parts of the input signal.
- Iterative Denoising: The denoising process is iterative. In each denoising step, the model makes a prediction of the less-noisy version of the latent representation, moving backward from z_T towards z. Skip connections in the U-Net help to preserve and refine details throughout this procedure.
- Decoding to Pixel Space: After the final denoising step, the now-denoised latent representation is decoded back into the sample space using a decoder $\mathcal{D}$, resulting in the reconstructed signal $\hat{X}$.
- Output: The output of the model is a new signal that retains the characteristics of the original input signal.

B. Signal Recovery Scheme

The signal recovery scheme can be divided into two phases, offline training phase and online recovery phase. Given the training data $\mathcal{X} = \left\{d_{k_s}^{(1)}, d_{k_s}^{(2)}, ..., d_{k_s}^{(n)}\right\}$ with n represent n-th training sample, we aim at decreasing the loss between the recovered signal $\hat{d}_{k_s}^{(n)}$ and the actual signal $d_{k_s}^{(n)}$ during the offline training phase. Thus, we define the following mean square error (MSE) loss function

$$MSE = \frac{1}{N}\sum_{n=1}^{N}\left\|d_{k_s}^{(n)} - \hat{d}_{k_s}^{(n)}\right\|^2 \tag{10}$$

TABLE I Simulation Parameters

Parameter	Value
U-Net contracting path kernel size	3×3
U-Net contracting path stride	1
U-Net expansive path kernel size	2×2
U-Net expansive path stride	2
Attention kernel size	2×2
Noise scheduling mechanism	Markov chain
Noise scheduling variance $\beta_1 - \beta_T$	0.0001 – 0.015
Noise distribution	Normal

Backpropagation is used during the training to update the diffusion model parameters θ. Given the trained model, we perform the online signal recovery with the given test data. The signal recovery procedure is illustrated in Algorithm 1

Algorithm 1 Diffusion Model-based Signal Recovery

Initialization: i

Offline training phase

Input training set $\mathcal{X}$
while $i \leq I$ **do**
  Update θ via backproagation.
  $i = i + 1$
end while
return $\mathcal{F}_\theta$

Online signal recovery phase

Input test samples
Output recovered signal $\hat{d}_{k_s}^{(n)}$ =0

where i and I are respectively the iteration index and the maximum number of iteration.

C. Training and Testing Setup

The entire process is trained end-to-end, with the goal of the denoising process to learn to reverse the diffusion process. Adam optimizer is used to optimize the network parameters. The learning rate is set to 0.0001, batch size is 64 and drop 0.3 is added to overcome overfitting. TABLE I includes the diffusion model parameters. The simulation parameters to generate the data are illustrated in TABLE II. The generated training data consists of 18000 samples which is divided into 16000 samples for training and 2000 samples for testing. Normalized mean square error (NMSE) is used as an evaluation metric.

IV. Experimental Results

In this section, we provide simulation results to evaluate the performance of the proposed diffusion model and testify its effectiveness and robustness. Simulation parameters are given in TABLE II. For sake of comparison, we use BRSnet with attention (BRSnetWA) in [13].

Fig. 3 compares the performance of the proposed diffusion model and BRSnet in terms NMSE. Both models employ attention mechanism to optimize learnable parameters by focusing on crucial features and preventing the loss of important features. Nevertheless, the location of deploying the attention plays a crucial role on the performance. Our proposed diffusion model incorporates the attention to focus on high quality features inside the U-Net and during the denoising procedure. This enhances the capability of the model in learning the useful features for noise and interference removal signal recovery.

TABLE II Simulation Parameters

Parameter	Value
Number of clusters	10
Number of LEO satellites per cluster	8
Number of SUs	100
Number of BSs	4
Number of antennas per satellite	64
Number of antennas per SU	8
Carrier frequency	28 GHz
Satellite antenna gain	35 dBi
User antenna gain	37 dBi
Scintillation loss	0.5 dB
Atmospheric loss	0.3 dB
Rician factor	2.8

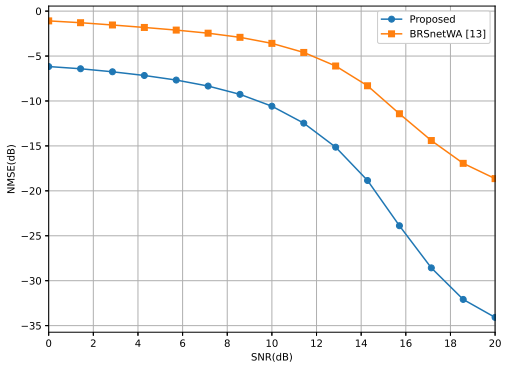

Fig. 3. NMSE versus SNR.

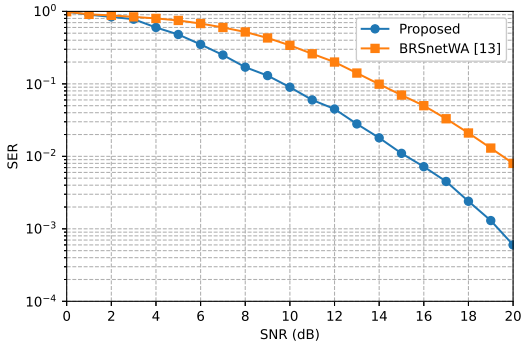

Fig. 4. NMSE versus SNR.

In addition to NMSE, we define symbol error rate (SER) metric as a performance metric. SER is defined as follows:

$$SER = \frac{1}{T} \sum_{t=1}^{T} \gamma_{d_k}^{(t)}, \tag{11}$$

where $\gamma_{d_k}^{(t)}$ is an indicator has value 1 when the predicted sample $\hat{d}_{k_s}$ is equal to the test sample d_{k_s} and 0 otherwise. T represents the total number of symbols.

The SER performance of the proposed diffusion model is depicted in Fig. 4. It can be observed that the proposed diffusion moded can remarkably improve the SER performance and a performance gap of around 4.1 dB between BRSnetWA and the proposed diffusion model-based scheme can be observed under moderate and high SNR conditions.

V. Conclusion

In this work, we proposed a diffusion model-based signal recovery scheme in coexisting satellite and terrestrial networks where LEO satellite constellation is modelled as cell-free MIMO and experiencing interference from the terrestrial network. We formulated the signal recovery problem and designed a diffusion model which leverages the denoising mechanism to recover the signals from noisy and distorted signals. Simulation results showed the superiority of the proposed model over the compared recent method.

References

[1] A. U. Rahman, M. A. Kishk, and M.-S. Alouini, "Coexistence of terrestrial and satellite networks in the 28-GHz band," *IEEE Trans. Aerosp. Electron. Syst.*, vol. 59, no. 6, pp. 8342–8354, 2023.

[2] L. Sormunen, H. Martikainen, J. Puttonen, and D. Panaitopol, "Coexistence of terrestrial and non-terrestrial networks on adjacent frequency bands," in *2022 11th Adv. Satell. Multimedia Syst. Conf. 17th Signal Process. Space Commun. Workshop (ASMS/SPSC)*, 2022, pp. 1–6.

[3] M. Vázquez, L. Blanco, and A. I. Pérez-Neira, "Spectrum sharing backhaul satellite-terrestrial systems via analog beamforming," *IEEE J. Sel. Topics Signal Process.*, vol. 12, no. 2, pp. 270–281, 2018.

[4] Q. Chen, Y. Zhang, Z. Zhou, Z. Wang, O. K. Jensen, G. F. Pedersen, and M. Shen, "Efficient digital signal recovery for satellite communications with active phased arrays," *IEEE Microw. Wireless Technol. Lett.*, vol. 33, no. 5, pp. 627–630, 2023.

[5] Y. Zhang, Z. Wang, Y. Huang, W. Wei, G. F. Pedersen, and M. Shen, "A digital signal recovery technique using DNNs for LEO satellite communication systems," *IEEE Trans. Ind. Electron.*, vol. 68, no. 7, pp. 6141–6151, 2021.

[6] Q. Chen, Y. Zhang, F. Jalili, Z. Wang, Y. Huang, Y. Wang, Y. Liu, G. F. Pedersen, and M. Shen, "Robust digital signal recovery for leo satellite communications subject to high SNR variation and transmitter memory effects," *IEEE Access*, vol. 9, pp. 135 803–135 815, 2021.

[7] Q. Li, L. Huang, W. Liu, X. Chen, and L. Feng, "Cold-start satellite signal acquisition aided by an antenna array in the presence of outliers," *IEEE Trans. Veh. Technol.*, vol. 72, no. 5, pp. 5847–5861, 2023.

[8] X. Kang, L. Liu, and H. Ma, "ESR-GAN: Environmental signal reconstruction learning with generative adversarial network," *Internet Things J.*, vol. 8, no. 1, pp. 636–646, 2021.

[9] H. Al-Hraishawi, J. ur Rehman, and S. Chatzinotas, "Quantum optimization algorithm for LEO satellite communications based on cell-free massive MIMO," in *2023 IEEE Inter. Conf. Commun. Workshops (ICC Workshops)*. IEEE, Oct. 2023, pp. 1759–1764.

[10] J.-B. Kim and I.-H. Lee, "Non-orthogonal multiple access in coordinated direct and relay transmission," *IEEE Commun. Lett.*, vol. 19, no. 11, pp. 2037–2040, Nov. 2015.

[11] T. Hou and A. Li, "Performance analysis of NOMA-RIS aided integrated navigation and communication (INAC) networks," *IEEE Trans. Veh. Technol.*, pp. 1–14, May 2023.

[12] L. You, K.-X. Li, J. Wang, X. Gao, X.-G. Xia, and B. Ottersten, "Massive MIMO transmission for LEO satellite communications," *IEEE J. Sel. Areas Commun.*, vol. 38, no. 8, pp. 1851–1865, Jun. 2020.

[13] X. Yu and D. Li, "Attention mechanism aided signal detection in backscatter communications with insufficient training data," *IEEE Trans. Veh. Technol.*, pp. 1–5, 2023.

[14] J. Ho, A. Jain, and P. Abbeel, "Denoising diffusion probabilistic models," *arXiv preprint arxiv:2006.11239*, 2020.

[15] A. Nichol and P. Dhariwal, "Improved denoising diffusion probabilistic models," *ArXiv*, vol. abs/2102.09672, 2021. [Online]. Available: https://api.semanticscholar.org/CorpusID:231979499